A TRUST REGION AGGRESSIVE SPACE MAPPING ALGORITHM FOR EM OPTIMIZATION

M.H. Bakr, J.W. Bandler, R.M. Biernacki, S.H. Chen and K. Madsen

SOS-97-9-R

November 1997

A TRUST REGION AGGRESSIVE SPACE MAPPING ALGORITHM FOR EM OPTIMIZATION

M.H. Bakr, J.W. Bandler, R.M. Biernacki, S.H. Chen and K. Madsen

Simulation Optimization Systems Research Laboratory
and Department of Electrical and Computer Engineering
McMaster University, Hamilton, Canada L8S 4L7

Tel 905 628 8228
Fax 905 628 8225
Email j.bandler@ieee.org

Abstract

A robust new algorithm for EM optimization of microwave circuits is presented. The algorithm integrates a trust region methodology with the aggressive space mapping (ASM) concept. The trust region ensures that each step taken results in improved alignment between the coarse and fine models needed to execute ASM. A new automated multi-point parameter extraction process is implemented. Waveguide transformer design, and EM optimization of a double-folded stub filter and of an HTS filter illustrate our new results.

SUMMARY

Introduction

A novel algorithm for aggressive space mapping (ASM) EM optimization [1] is introduced. Space mapping aims at aligning two different simulation models: a "coarse" model, typically an empirical circuit simulation and a "fine" model, typically a full wave EM simulation. The technique combines the accuracy of the fine model with the speed of the coarse model.

This work was supported in part by Optimization Systems Associates Inc. (before acquisition by HP EEsof) and in part by the Natural Sciences and Engineering Research Council of Canada under Grants OGP0007239 and OGP0042444 and through the Micronet Network of Centres of Excellence. M.H. Bakr is funded by TRIO through a student internship.

K. Madsen is with the Institute of Mathematical Modeling, Technical University of Denmark, DK-2800 Lyngby, Denmark.

Parameter extraction is a crucial part of the technique. In this step the parameters of the coarse model whose response matches the fine model response is obtained. The extracted parameters may not be unique, causing the technique to fail to converge to the optimal design.

Recently, a multi-point parameter extraction concept was proposed [2] to enhance the uniqueness of the extraction step at the expense of an increased number of fine model simulations. The selection of points was arbitrary, not automated and no information about the mapping between the two spaces was taken into account.

Our proposed ASM algorithm automates the selection of fine model points used for the multi-point parameter extraction step. An iterative approach utilizes all the fine model points simulated since the last successful iteration in the multi-point parameter extraction. Also, the current approximation to the mapping between the two spaces is integrated into the parameter extraction step.

The step taken at each iteration is constrained by a suitable trust region [3]. The size of this trust region is modified according to the match between the actual reduction in the misalignment between the two spaces and the predicted reduction in the misalignment. This ensures that the alignment between the two spaces is improved in each iteration.

The New Algorithm

At the *i*th iteration, the error vector $\boldsymbol{f}^{(i)} = \boldsymbol{P}(\boldsymbol{x}_{em}^{(i)}) - \boldsymbol{x}_{os}^{*}$ defines the difference between the vector of extracted coarse model parameters $\boldsymbol{x}_{os}^{(i)} = \boldsymbol{P}(\boldsymbol{x}_{em}^{(i)})$ and the optimal coarse model design $\boldsymbol{x}_{os}^{*}$ in the "*os*" space. Subscript "*em*" identifies the fine model space, $\boldsymbol{P}$ denotes the mapping function. The mapping between the two models is established if this error vector is driven to zero. So, the value $\left\| \boldsymbol{f}^{(i)} \right\|$ can serve as a measure of the misalignment between the two spaces in the *i*th iteration. The step taken in the *i*th iteration is given by

$$(\boldsymbol{B}^{(i)T}\boldsymbol{B}^{(i)} + l\,\boldsymbol{I})\,\boldsymbol{h}^{(i)} = -\boldsymbol{B}^{(i)T}\boldsymbol{f}^{(i)} \qquad (1)$$

where $\boldsymbol{B}^{(i)}$ is an approximation to the Jacobian of the coarse model parameters with respect to the fine model parameters at the *i*th iteration. The parameter l is selected such that the step obtained satisfies $\left\|\boldsymbol{h}^{(i)}\right\| \leq d$, where d is the size of the trust region. This is done utilizing the iterative algorithm suggested in [3]. The candidate point for the next iteration is $\boldsymbol{x}_{em}^{(i+1)} = \boldsymbol{x}_{em}^{(i)} + \boldsymbol{h}^{(i)}$. Single point parameter extraction is then applied at the point $\boldsymbol{x}_{em}^{(i+1)}$ to get $\boldsymbol{f}^{(i+1)} = \boldsymbol{P}(\boldsymbol{x}_{em}^{(i+1)}) - \boldsymbol{x}_{os}^{*}$. The point $\boldsymbol{x}_{em}^{(i+1)}$ is accepted if it satisfies a success criterion related to a reduction in the ℓ_2 norm of the vector $\boldsymbol{f}$. Then the matrix $\boldsymbol{B}^{(i)}$ is updated using Broyden's formula [4]. Otherwise, the validity of the extraction process leading to $\boldsymbol{f}^{(i+1)}$ at the suggested point $\boldsymbol{x}_{em}^{(i+1)}$ is suspect. The residual error $\boldsymbol{f}^{(i+1)}$ is then used to construct a candidate step from the point $\boldsymbol{x}_{em}^{(i+1)}$ by using (1). The new point is then added to the set of points employed for simultaneous parameter extraction: a new value for $\boldsymbol{f}^{(i+1)}$ is obtained by solving

$$\underset{\boldsymbol{x}_{os}}{minimize} \left\| \boldsymbol{R}_{os}(\boldsymbol{x}_{os} + \boldsymbol{B}^{(i)}(\boldsymbol{x}_{em} - \boldsymbol{x}_{em}^{(i+1)}) - \boldsymbol{R}_{em}(\boldsymbol{x}_{em}) \right\|, \tag{2}$$

simultaneously for all $\boldsymbol{x}_{em} \in V$, where V is the set of fine model points used for multi-point parameter extraction. Thus, the extracted vector of coarse model parameters is obtained by matching the responses of the two models at a number of points in the parameter space. Also, it is clear from (2) that a perturbation in the fine model space of $\Delta\boldsymbol{x}_{em}$ corresponds to a perturbation in the coarse model space of $\boldsymbol{B}^{(i)}\Delta\boldsymbol{x}_{em}$. This is logical since the matrix $\boldsymbol{B}^{(i)}$ represents the most up-to-date approximation to the mapping between the two spaces. Thus, the available information about the mapping between the two space is exploited.

The new extracted coarse model parameters either satisfy the success criterion or they are used to predict another candidate point which is then added to the set of points used for parameter extraction and the whole process is repeated. See Fig. 1. Using this recursive multi-point parameter extraction process improves the accuracy. This may lead to the satisfaction of the success criterion or the step is declared a

failure. The step failure is declared in one of two cases: either the vector of extracted parameters approaches a limiting value with the success criterion not satisfied, or the number of fine model simulations since the last successful iteration has reached (n+1). In the first case, the extracted coarse model parameters are trusted and the accuracy of the linearization used to predict $\boldsymbol{h}^{(i)}$ is suspected. Thus to ensure a successful step from the current point $\boldsymbol{x}_{em}^{(i)}$, the trust region size is shrunk and a new suggested point $\boldsymbol{x}_{em}^{(i+1)}$ is obtained. In the latter case, sufficient information is available to obtain an estimate for the Jacobian of the fine model responses with respect to the fine model parameters. This is done by solving the system of linear equations

$$\begin{pmatrix} (\boldsymbol{x}_{em}^{(i)} - \boldsymbol{x}_{em}^{(i+1)})^T \\ (\boldsymbol{x}_{em}^{(i)} - \boldsymbol{x}_t^{(1)})^T \\ \vdots \\ (\boldsymbol{x}_{em}^{(i)} - \boldsymbol{x}_t^{(n-1)})^T \end{pmatrix} (\boldsymbol{J})^T = \begin{pmatrix} (\boldsymbol{g}^{(i)} - \boldsymbol{g}^{(i+1)})^T \\ (\boldsymbol{g}^{(i)} - \boldsymbol{g}_t^{(1)})^T \\ \vdots \\ (\boldsymbol{g}^{(i)} - \boldsymbol{g}_t^{(n-1)})^T \end{pmatrix}, \tag{3}$$

where $\boldsymbol{x}_t^{(k)}$ is the kth candidate point used for multi-point parameter extraction and $\boldsymbol{g}_t^{(k)}$ is the corresponding error between the fine model responses and the optimal coarse model responses. This matrix is then used to make a step $\boldsymbol{h}^{(i)}$ in the parameter space by solving the system of equations

$$(\boldsymbol{J}^T \boldsymbol{J} + l \boldsymbol{I}) \boldsymbol{h}^{(i)} = -\boldsymbol{J}^T \boldsymbol{g}^{(i)}, \tag{4}$$

varying parameter l until $\|\boldsymbol{h}^{(i)}\| \le \boldsymbol{d}$. If there is no reduction in the l_2 norm of the vector function $\boldsymbol{g}$, the trust region is shrunk and (4) is resolved. This is repeated until either the size of the trust region has shrunk significantly and hence the algorithm terminates or a successful step is taken. This successful step is then used instead of the step obtained by (1) and the algorithm proceeds.

Double-folded Stub Filter

We consider the design of the double-folded stub (DFS) microstrip structure shown in Fig. 2 (Bandler *et al.* [5,6,7]). Folding the stubs reduces the filter area w.r.t. the conventional double stub structure (Rautio [8]). The filter is characterized by five parameters : W_1 , W_2 , S, L_1 and L_2 (see Fig. 2).

L_1, L_2 and S are chosen as optimization variables. W_1 and W_2 are fixed at 4.8 mil. The design specifications are given by $|S_{21}| \geq$ -3 dB in the passband and $|S_{21}| \leq$ -30 dB in the stopband, where the passband includes frequencies below 9.5 GHz and above 16.5 GHz and the stopband lies in the range [12 GHz, 14 GHz]. The structure is simulated by Sonnet's ***em*** [9] through OSA's Empipe [10]. The coarse model is a coarse-grid ***em*** model with cell size 4.8 mil by 4.8 mil. The fine model is a fine-grid ***em*** model with cell size 1.6 mil by 1.6 mil. Other parameters are summarized in Table I.

Table II shows the optimal coarse model parameters obtained by the OSA90/hope [10] minimax optimizer. Fig. 3 shows the response along with the fine model ***em*** response evaluated using the optimal coarse model parameters. The time needed to simulate the structure (coarse model) at a single frequency is only 5 CPU seconds on a Sun SPARCstation 10. This includes the automatic response interpolation carried out to accommodate off-grid geometries.

It is clear from Fig. 3 that the fine model response violates the design specifications at the starting point. The new ASM technique required only two iterations to reach the solution. The algorithm's progress is shown in Table III. The number of required fine model simulations is 17. Most of these simulations were needed for response interpolation. The response of the fine model at the solution is shown in Fig. 4. The CPU time needed for the fine model is approximately 70 seconds per frequency point.

Waveguide Transformer

We optimized a two-section waveguide transformer as shown in Fig. 5. This example is a classical microwave circuit design problem [11] and is presented to illustrate the new ASM algorithm. Here we use two empirical models: an ideal model which neglects the junction discontinuities and a nonideal model which includes the junction discontinuity effects [11].

The ideal (coarse) model is first optimized. The results are shown in Table IV. The optimum ideal model response is shown in Fig. 6 along with the nonideal model response at the same point. Our algorithm terminated in three iterations, requiring 5 fine model simulations. The optimal nonideal model

design is given in Table V. The corresponding nonideal model response is shown in Fig. 7. This example is known to have more than one minimum for the parameter extraction step [2]. However, our new algorithm converged successfully to the optimal design. The number of simulations needed to align the two models is smaller than that reported in [2].

HTS Filter

We consider optimization of a high-temperature superconducting (HTS) filter [1,12]. This filter is illustrated in Fig. 8. The specifications are $|S_{21}| \geq 0.95$ in the passband and $|S_{21}| \leq 0.05$ in the stopband, where the stopband includes frequencies below 3.967 GHz and above 4.099 GHz and the passband lies in the range [4.008 GHz, 4.058 GHz]. The design variables for this problem are L_1, L_2, L_3, S_1, S_2 and S_3. We take L_0 = 50 mil and W = 7 mil. The coarse model exploits the empirical models of microstrip lines, coupled lines and open stubs available in OSA90/hope. The fine model employs a fine-grid ***em*** simulation. The material and physical parameters values used in both OSA90/hope and in ***em*** are shown in Table VI. The coarse model is first optimized using the OSA90/hope minimax optimizer. The optimal coarse model design is given in Table VII. The fine model response at the optimal coarse model design are shown in Fig. 9. The parameter extraction for this problem has several solutions. Fig. 10 shows how two of the extracted coarse model parameters changed with the number of points used for parameter extraction. The first point (1) is obtained using normal parameter extraction. These extracted values would have caused the original ASM technique to diverge. The new technique automatically generates a candidate point which is then used together with the original point to carry out a multi-point parameter extraction and the second point (2) is obtained. To confirm that this point is the required one a third candidate point is automatically generated and the extraction is repeated using the three points to obtain the third extracted point (3). The second and third extracted points show that the extracted vector of coarse model parameters is approaching a limiting value and can thus be trusted. The coarse model response corresponding to the three extracted points of Fig. 10 are shown in Fig. 11.

For the remaining iterations, single point parameter extraction worked well. The fine model responses and the coarse model responses for the corresponding extracted points are shown in Fig. 12. The optimal fine model design was obtained in 5 iterations which required 8 fine model simulations. The optimal fine model design is given in Table VIII. The fine model response at this design is shown in Fig. 13. The passband ripples are shown in Fig. 14.

In the original space mapping approaches [1,12] this example required significant manual intervention to successfully complete the parameter extraction phase. Furthermore, without such intervention the previous approaches would not work.

Conclusions

A powerful new algorithm implementing the aggressive space mapping technique is introduced. It aims at automatically improving the uniqueness of the parameter extraction step, the most critical step in the space mapping process, and exploiting all available fine model simulations. Through examples which have proved difficult in the past we show that the new ASM algorithm automatically overcomes the nonuniqueness of the parameter extraction step in a logical way. We are currently testing the proposed algorithm using HP HFSS [13].

References

[1] J.W. Bandler, R.M. Biernacki, S.H. Chen, R.H. Hemmers and K. Madsen, "Electromagnetic optimization exploiting aggressive space mapping," *IEEE Trans. Microwave Theory Tech.*, vol. 43, 1995, pp. 2874-2882.

[2] J.W. Bandler, R.M. Biernacki and S.H. Chen, "Fully automated space mapping optimization of 3-D structures," in *IEEE MTT-S int. Microwave Symp. Dig.* (San Francisco, CA), 1996, pp. 753-756.

[3] J.J. Mor and D.C. Sorenson, "Computing a trust region step," *SIAM J. Sci. Stat. Comp.*, vol. 4, 1983, pp. 553-572.

[4] C.G. Broyden, "A class of methods for solving nonlinear simultaneous equations," *Math. Comp.*, vol. 19, 1965, pp. 577-593.

[5] J.W. Bandler, R.M. Biernacki, S.H. Chen, P.A. Grobelny and R.H. Hemmers, "Space mapping technique for electromagnetic optimiztion," *IEEE Trans. Microwave Theory Tech.*, vol. 42, 1994, pp. 2536-2544.

[6] J.W. Bandler, R.M. Biernacki, S.H. Chen, P.A. Grobelny and R.H. Hemmers, "Exploitation of coarse grid for electromagnetic optimization," *IEEE MTT-S Int. Microwave Symp. Dig* (San Diego, CA), 1994, pp. 381-384.

[7] J.W. Bandler, R.M. Biernacki, S.H. Chen, D.G. Swanson, Jr. and S. Ye, "Microstrip filter design using direct EM field simulation," *IEEE Trans. Microwave Theory Tech*., vol. 42, 1994, pp. 1353-1359.

[8] J.C. Rautio, Sonnet Software, Inc., 1020 Seventh North Street, Suite 210, Liverpool, NY 13088, Private Communication, 1992.

[9] ***em***™ , Sonnet Software, Inc., 1020 Seventh North Street, Suite 210, Liverpool, NY 13088, 1996.

[10] OSA90/hope™ and Empipe™, Optimization Systems Associates Inc., Ontario, Canada, 1997.

[11] J.W. Bandler, "Computer optimization of inhomogeneous waveguide transformers," *IEEE Trans. Microwave Theory Tech*., vol. MTT-17, 1969, pp. 563-571.

[12] J.W. Bandler, R.M. Biernacki, S.H. Chen, W.J. Gestinger, P.A. Grobelny, C. Moskowitz and S.H. Talisa, "Electromagnetic design of high-temperature superconducting filters," *Int. J. Microwave and Millimeter-Wave Computer-Aided Engineering*, vol. 5, 1995, pp. 331-343.

[13] *HFSS*, Hewlett-Packard Co., 1400 Fountaingrove Parkway, Santa Rosa, CA 95403, 1997.

TABLE I
MATERIAL AND PHYSICAL PARAMETERS FOR THE COARSE AND FINE ***em*** MODELS OF THE DFS FILTER

Model Parameter	Value
substrate dielectric constant	9.9
substrate thickness (mil)	5
shielding cover height (mil)	∞
conducting material thickness	3.0E-6
substrate dielectric loss tangent	2.0E-3
resistivity of metal (Ωm)	1.72E-8
magnetic loss tangent	0
surface reactance (Ω/sq)	0
lower frequency limit (GHz)	5
upper frequency limit (GHz)	20
frequency increment size (GHz)	0.25

TABLE II
OPTIMAL DESIGN OF THE COARSE MODEL FOR THE DFS FILTER

Parameter	Value (mil)
L_1	88.8
L_2	84.1
S	3.9

TABLE III
VALUES OF DESIGNABLE PARAMETERS AT EACH ITERATION FOR THE DFS FILTER

Parameter	$\boldsymbol{x}_{em}^{0}$	$\boldsymbol{x}_{em}^{1}$	$\boldsymbol{x}_{em}^{2}$
L_1	88.8	89.5	94.3
L_2	84.1	84.6	85.4
S	3.9	4.7	4.7
all values are in mils			

TABLE IV
OPTIMAL DESIGN OF THE COARSE (IDEAL) MODEL
FOR THE TWO-SECTION WAVEGUIDE TRANSFORMER

Parameter	Value (cm)
a_1	0.712
b_1	1.395
a_2	1.657
b_2	1.590

TABLE V
VALUES OF OPTIMIZABLE PARAMETERS
AT EACH ITERATION OF THE NEW ASM TECHNIQUE
FOR THE TWO-SECTION WAVEGUIDE TRANSFORMER

Parameter	$\boldsymbol{x}_{em}^{0}$	$\boldsymbol{x}_{em}^{1}$	$\boldsymbol{x}_{em}^{2}$	$\boldsymbol{x}_{em}^{3}$
a_1	0.712	0.715	0.716	0.716
b_1	1.395	1.400	1.402	1.402
a_2	1.657	1.591	1.560	1.560
b_2	1.590	1.541	1.518	1.518
all values are in cm				

TABLE VI
MATERIAL AND PHYSICAL PARAMETERS
FOR THE HTS FILTER

Model Parameter	OSA90/hope	***em***
substrate dielectric constant	23.425	23.425
substrate thickness (mil)	19.9516	19.9516
shielding cover height (mil)	∞	250
conducting material thickness	1.968E-2	0
substrate dielectric loss tangent	3.0E-5	3.0E-5
resistivity of metal (Ωm)	0	4.032E-8
surface roughness of metal	0	—
magnetic loss tangent	—	0
surface reactance (Ω/sq)	—	0
x-grid cell size (mil)	—	1.00
y-grid cell size (mil)	—	1.75

TABLE VII
THE OPTIMAL DESIGN OF THE COARSE MODEL
FOR THE HTS FILTER

Parameter	Optimal Value (mil)
L_1	188.33
L_2	197.98
L_3	188.58
S_1	21.97
S_2	99.12
S_3	111.67

TABLE VIII
THE INITIAL AND FINAL DESIGNS OF THE FINE MODEL
FOR THE HTS FILTER

Parameter	Initial Value (mil)	Final Value (mil)
L_1	188.33	181.43
L_2	197.98	200.51
L_3	188.58	180.49
S_1	21.97	19.44
S_2	99.12	80.52
S_3	111.67	83.41

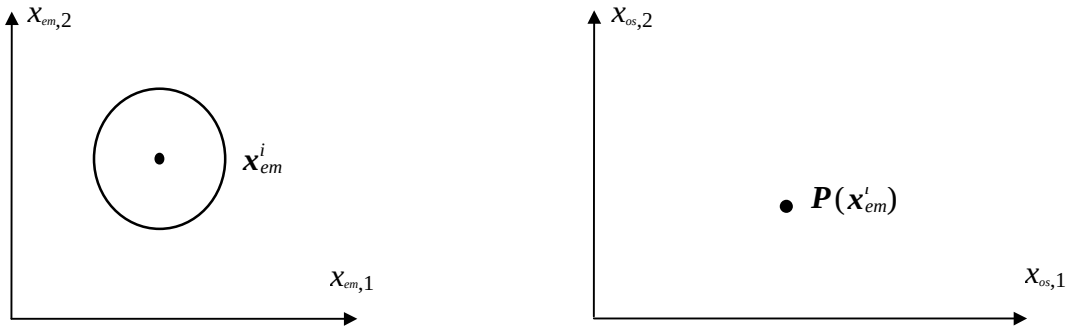

the current state at the *i*th iteration

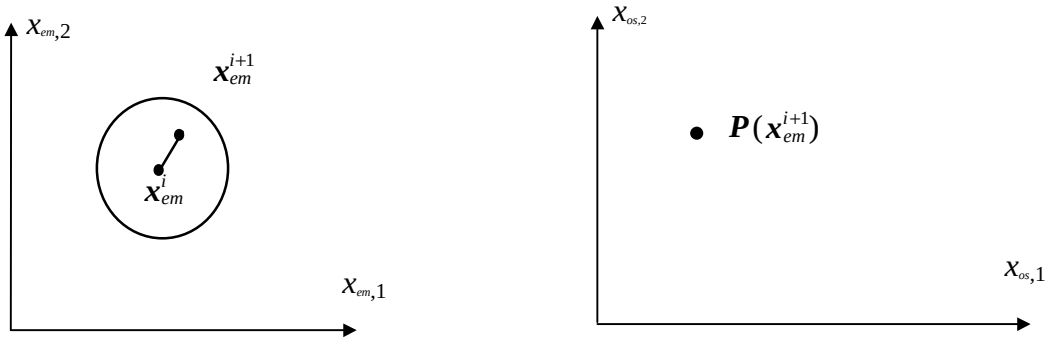

initial parameter extraction at the suggested point $\boldsymbol{x}_{\boldsymbol{em}}^{\boldsymbol{i+1}}$.

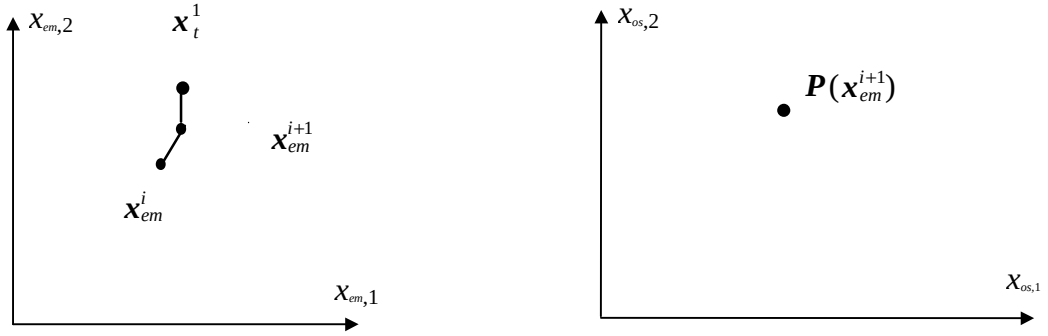

parameter extraction fails; an additional point $\boldsymbol{x}_{t}^{1}$ is obtained and multi-point parameter extraction is carried out to sharpen the solution

Fig. 1. Illustration of the automated multi-point parameter extraction.

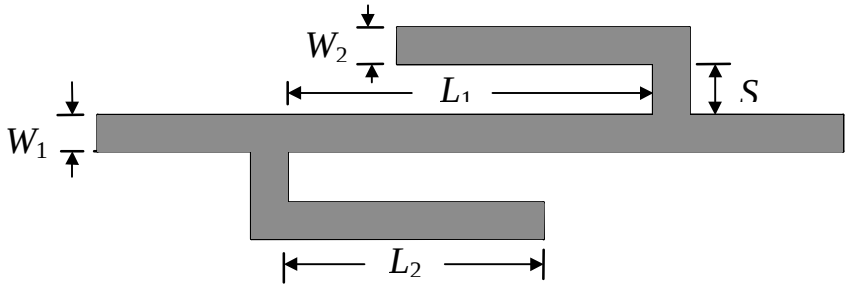

Fig. 2. The DFS filter [8].

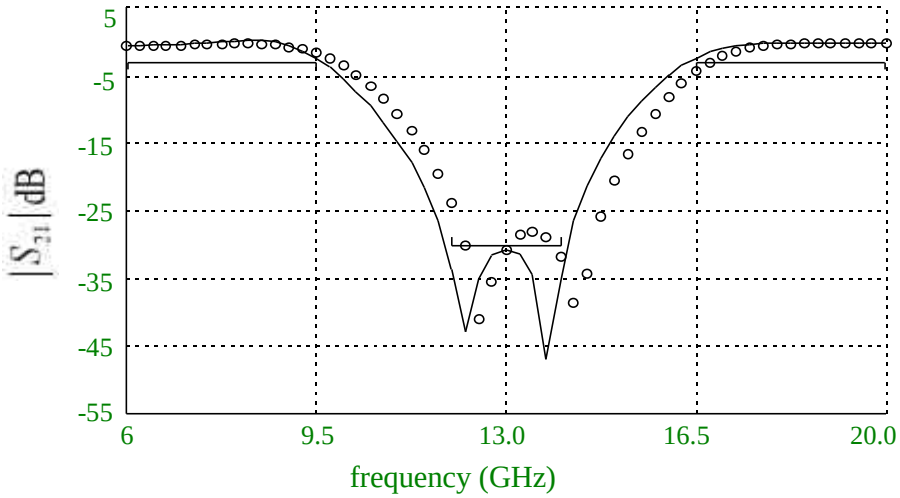

Fig. 3. The optimal coarse model response (—) and the fine model response (o) at the starting point for the DFS filter .

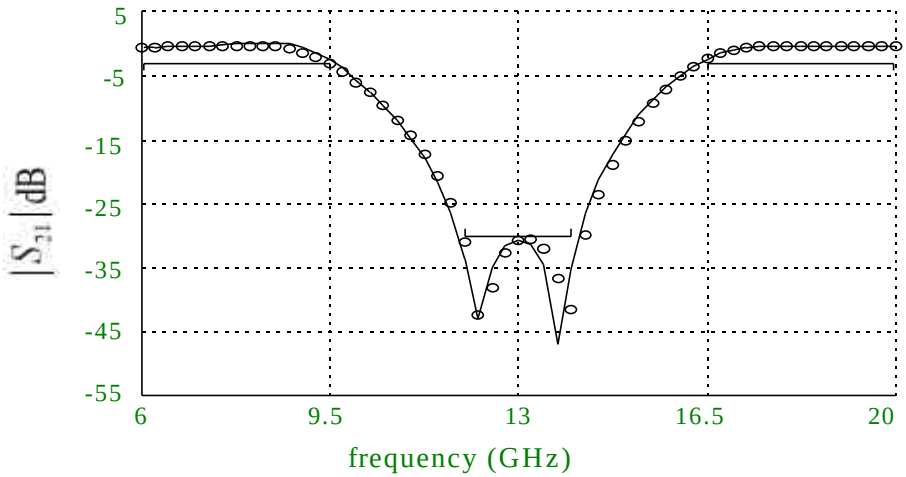

Fig. 4. The optimal coarse model response (—) and the optimal fine model response (o) for the DFS filter.

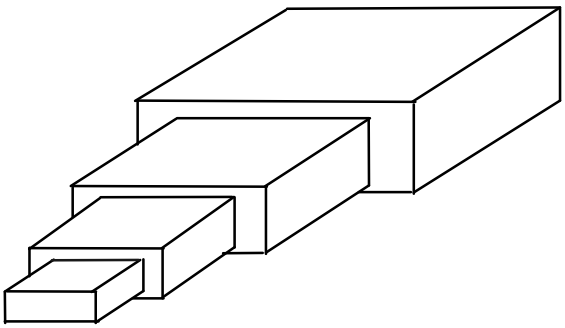

Fig. 5. A typical two-section waveguide transformer.

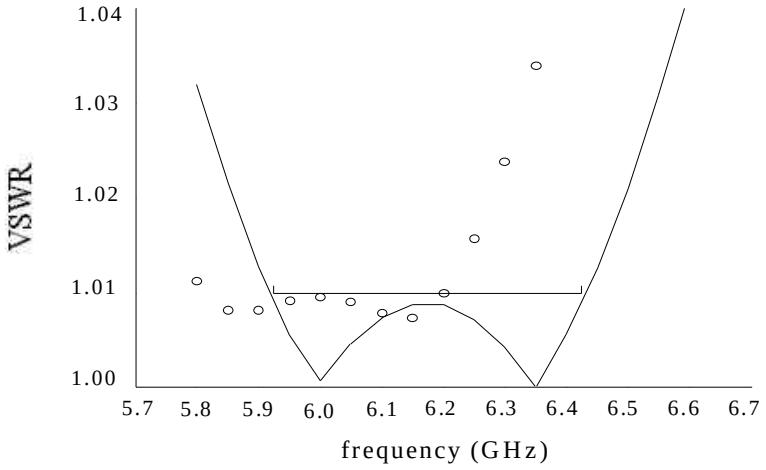

Fig. 6. The optimal coarse model response (—) and the fine model response (o) at the starting point for the two-section waveguide transformer.

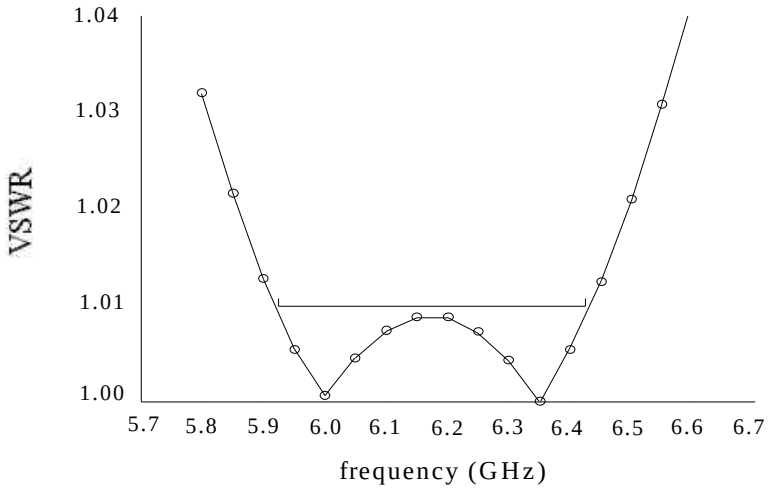

Fig. 7. The optimal coarse model response (—) and the optimal fine model response (o) for the two-section waveguide transformer.

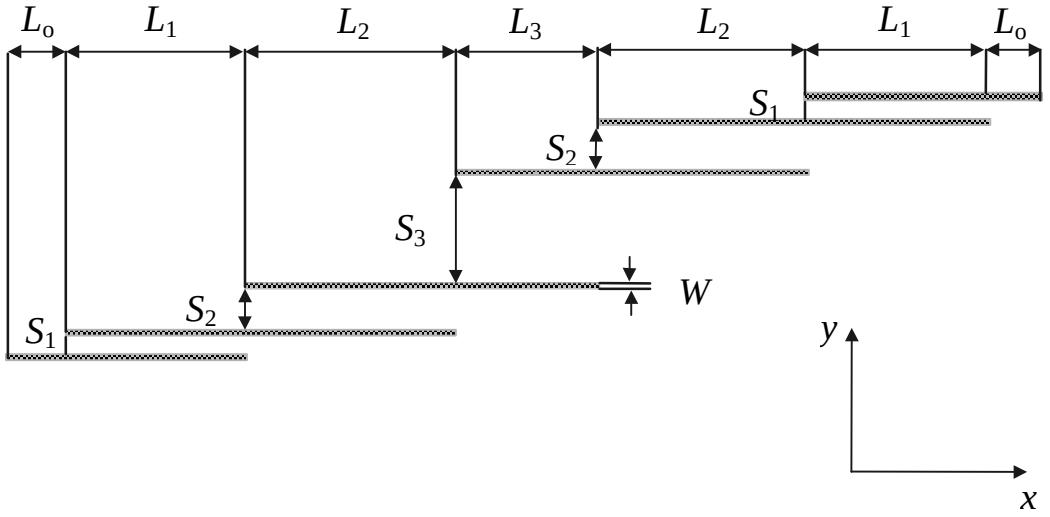

Fig. 8. The structure of the HTS filter [12].

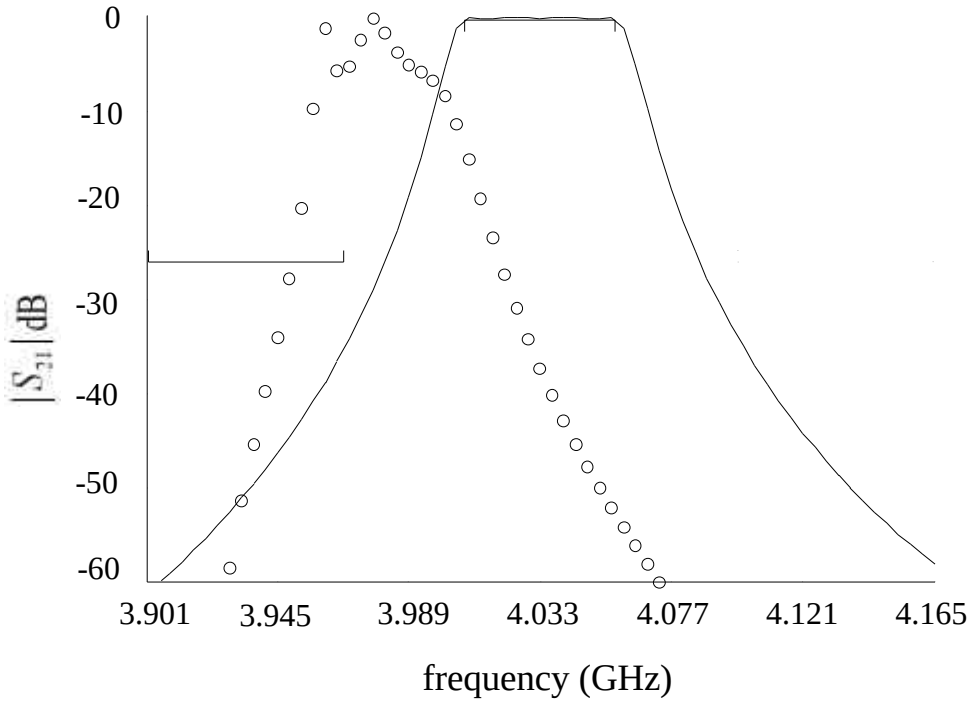

Fig. 9. The optimal coarse model response (—) and the fine model response (o) at the starting point for the HTS filter.

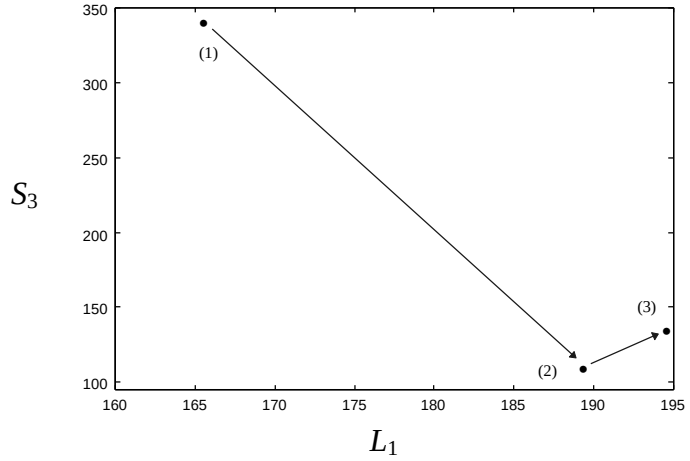

Fig. 10. The variation of two of the extracted coarse model parameters in the first iteration with the number of points used for parameter extraction where (1) is obtained using a single fine model point, (2) is obtained using two fine model points and (3) is obtained using three fine model points.

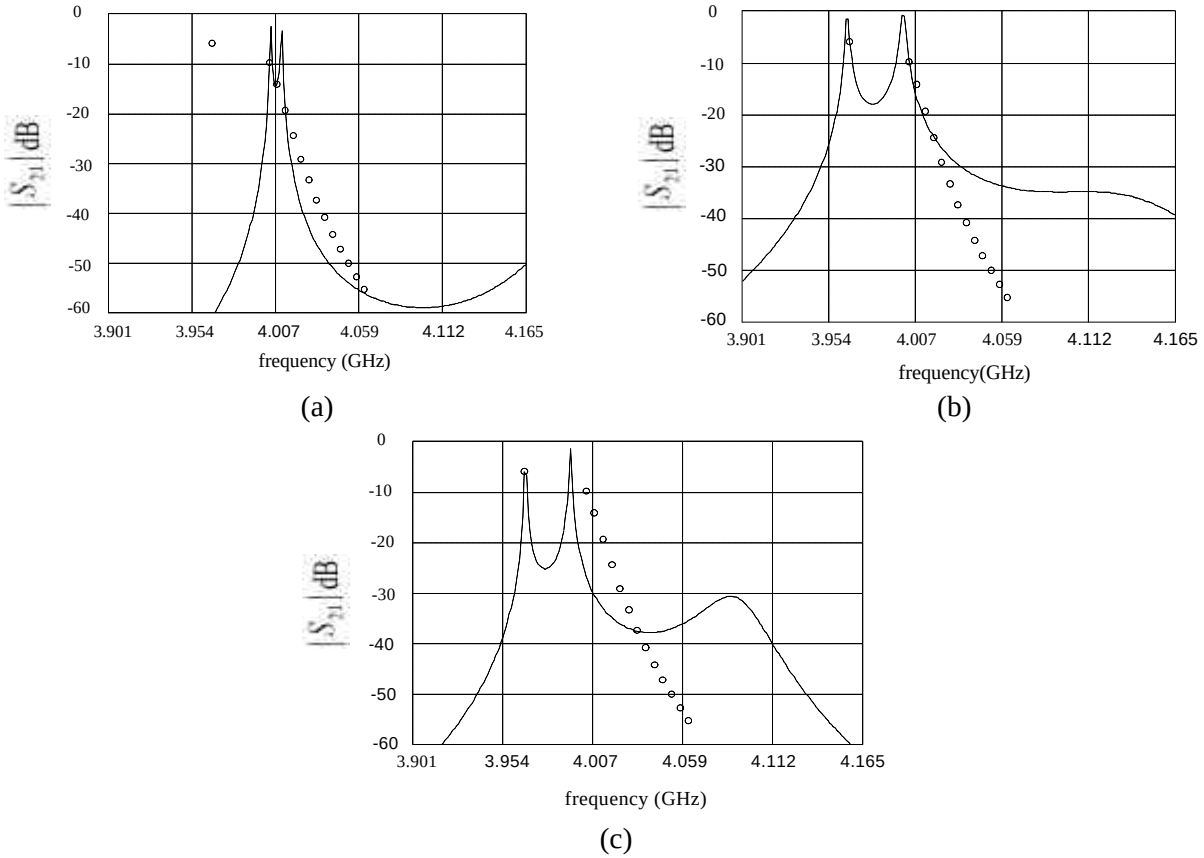

Fig. 11. The coarse model response (—) and the fine model response (o) corresponding to the three extracted points in Fig. 10 where (a) is obtained using a single fine model, (b) is obtained using two fine model points and (c) is obtained using three fine model points.

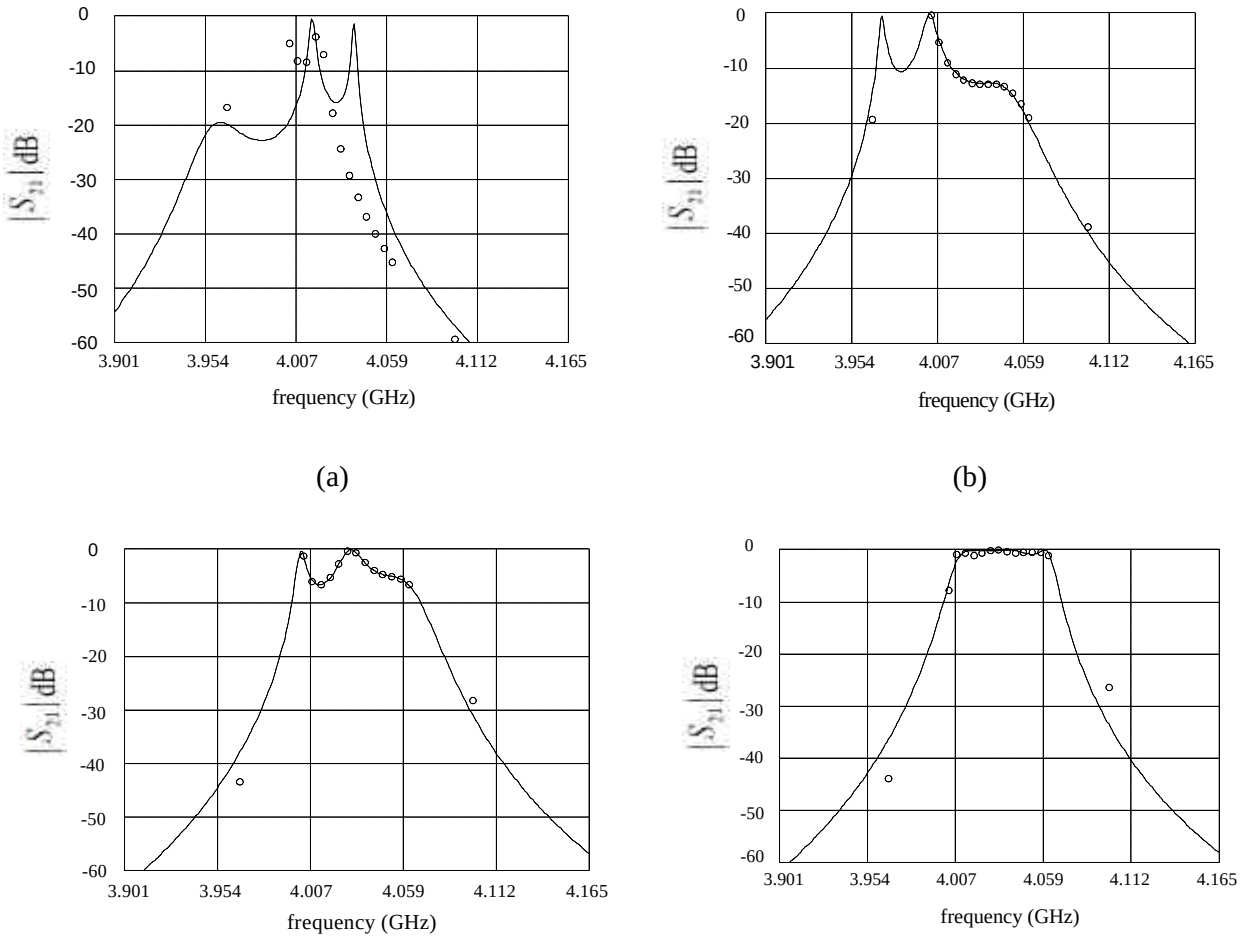

Fig. 12. The coarse model response (—) at the extracted point and the fine model response (o) corresponding to the second, third, fourth and fifth iterations.

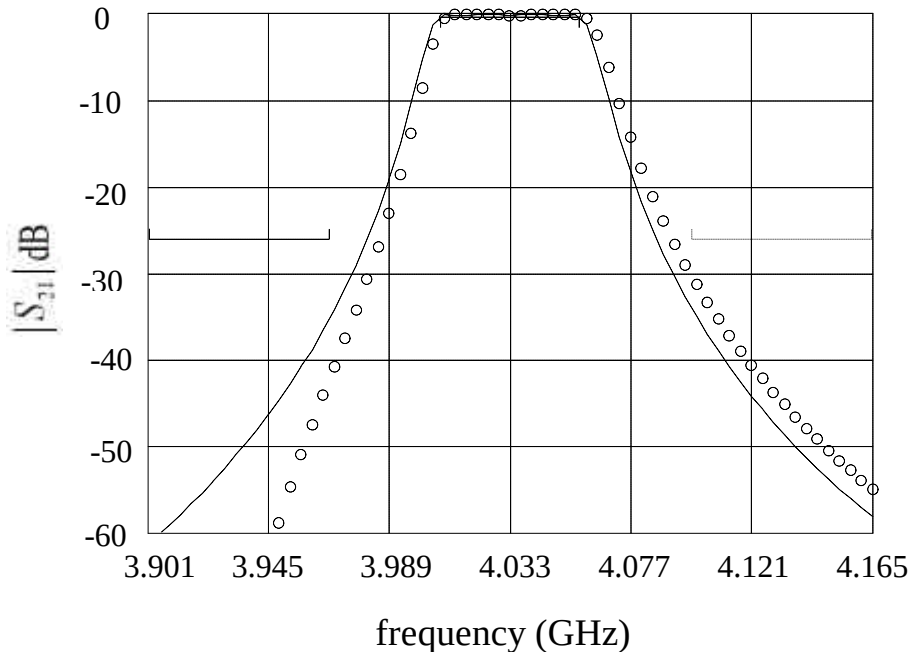

Fig. 13. The optimal coarse model response (—) and the optimal fine model response (o) for the HTS filter.

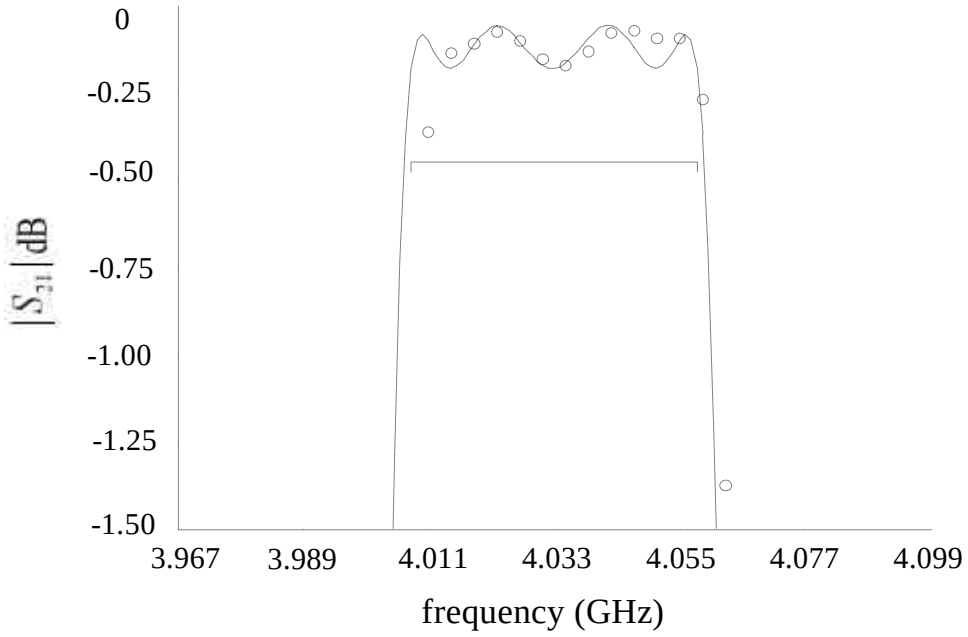

Fig. 14. The optimal coarse model response (—) and the optimal fine model response (o) for the HTS filter in the passband.